

## Lipid droplets of neuroepithelial cells are a major calcium storage site during neural tube formation in chick and mouse embryos<sup>1</sup>

K. T. Bush, H. Lee and R. G. Nagele

*Department of Molecular Biology, University of Medicine and Dentistry of New Jersey, School of Osteopathic Medicine, Stratford (New Jersey 08084, USA), and Department of Biology, Rutgers University, Camden (New Jersey 08102, USA)*

*Received 9 July 1991; accepted 27 November 1991*

**Abstract.** In situ precipitation of calcium ( $\text{Ca}^{2+}$ ) with fluoride and antimonate shows that  $\text{Ca}^{2+}$ -specific precipitate is localized almost exclusively within lipid droplets of neuroepithelial cells during neural tube formation in chick and mouse embryos. The density of  $\text{Ca}^{2+}$  precipitate within lipid droplets is generally greater in the apical ends of cells situated in regions of the neuroepithelium that are actively engaged in bending. These findings suggest that lipid droplets, in addition to providing a source of metabolic fuel for developing neuroepithelial cells, also serve as  $\text{Ca}^{2+}$ -storage and -releasing sites during neurulation.

**Key words.** Lipid; neuroepithelial cells; calcium; neurulation; neural tube; chick embryo; mouse embryo.

Several lines of evidence have implicated the calcium ion ( $\text{Ca}^{2+}$ ) as a key factor in regulating many types of cellular and morphogenetic movements, particularly those depending on microfilaments and the interactions of actin and myosin<sup>2–6</sup>. During the formation of the neural tube (NT), neuroepithelial (NE) cells possess prominent actin- and myosin-containing microfilament bundles at their apical (future luminal) ends<sup>7–9</sup>. The strategic location and orientation of these microfilaments and their association with local changes in the geometry of NE cells have led to the proposal that they contribute to the motive forces that bend the neuroepithelium during NT formation. The fact that experimental perturbations of free  $\text{Ca}^{2+}$  levels can influence the rate and extent of NT formation suggests that  $\text{Ca}^{2+}$  plays a key role in regulating this important developmental event<sup>10–14</sup>. For  $\text{Ca}^{2+}$  to serve in this capacity, NE cells must have a means to transiently store and release  $\text{Ca}^{2+}$  and control its local intracellular level. However, the structural identity of  $\text{Ca}^{2+}$ -storage and -releasing sites within NE cells and the mechanism by which  $\text{Ca}^{2+}$  is mobilized during sequential phases of NT formation remain unclear. As part of our interest in elucidating the regulatory role of  $\text{Ca}^{2+}$  in this process, we used a cytochemical technique developed by Poenie and Epel<sup>15</sup> to determine the intracellular distribution of  $\text{Ca}^{2+}$  in the neuroepithelium during various phases of NT formation in chick and mouse embryos.

### Materials and methods

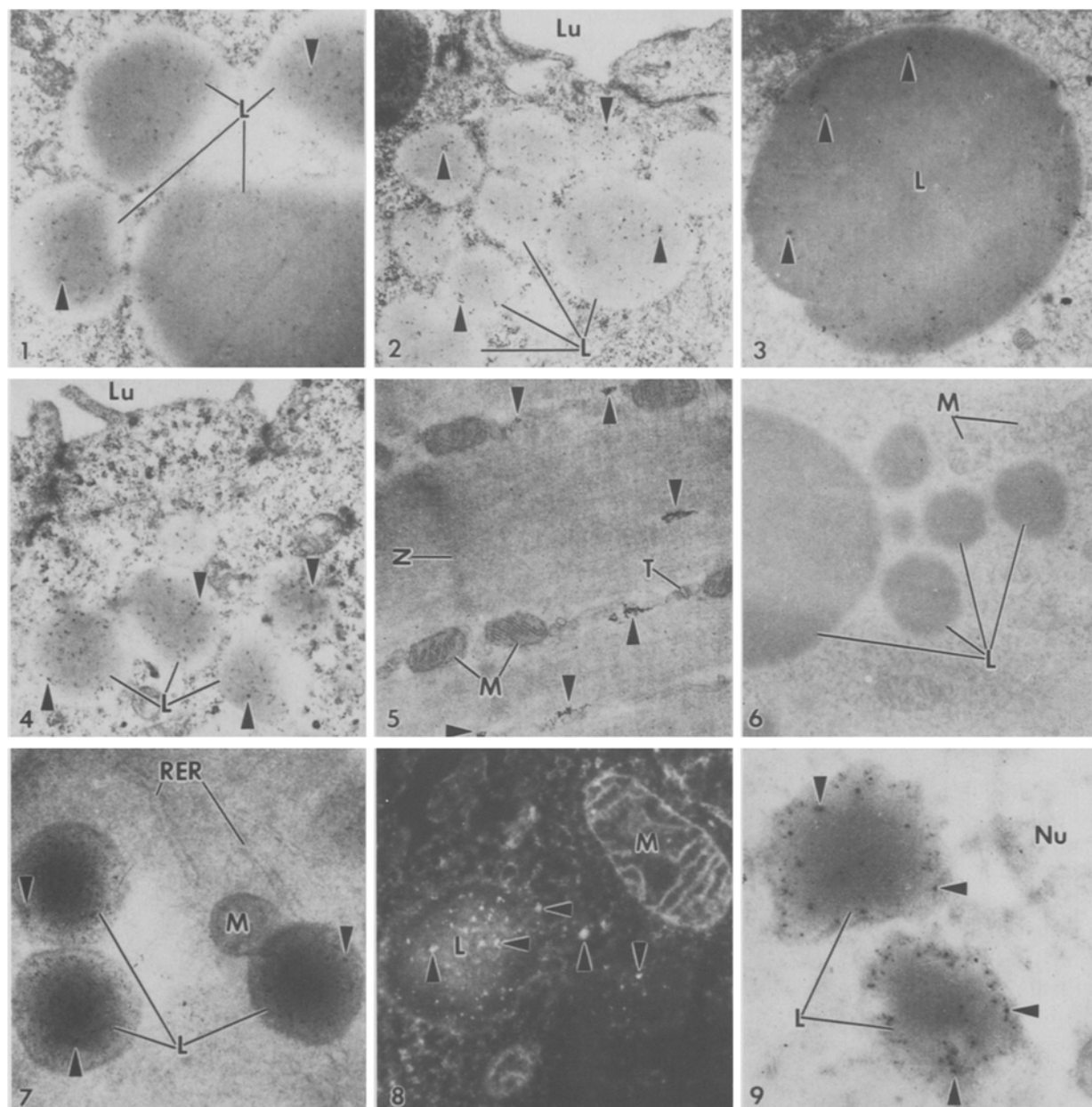
Stages 5–9 chick embryos<sup>16</sup> exhibiting successive phases of NT formation were procured by incubating fertile White Leghorn eggs at 37.5 °C. To obtain mouse embryos, random bred CD-1 mice (Charles River Laboratories) were paired for 2–3 h in the early morning and females were examined for the presence of a vaginal plug. The mice were sacrificed by cervical dislocation on days 8–10 of pregnancy. For the ultrastructural localization of  $\text{Ca}^{2+}$ , embryos were processed according to the fluoride-antimonate technique of Poenie and Epel<sup>15</sup> and

then prepared for routine transmission electron microscopy<sup>7</sup>. Some thin sections were contrasted with uranyl acetate and lead citrate; others were left uncontrasted to facilitate visualization of the electron-dense,  $\text{Ca}^{2+}$ -specific precipitate against a background with low overall contrast. Thin sections were examined and photographed with a Zeiss EM 109 electron microscope. In addition, thick (1  $\mu\text{m}$ ), unstained sections were mounted on 200-mesh copper grids, examined, and photographed using a Zeiss CEM 902 electron microscope equipped with an electron spectroscopic imaging system. To test the reaction specificity, mouse skeletal muscle tissue was processed for  $\text{Ca}^{2+}$  localization and used as a positive control. In addition, some embryos prepared for  $\text{Ca}^{2+}$  localization were subsequently treated with ethylene-glycol-bis (p-aminoethyl ether) N,N'-tetraacetic acid (EGTA) in distilled water (pH adjusted to 7.4) for 2 h at 4 °C before processing for electron microscopy.

Morphometry was used to measure (1) the density of  $\text{Ca}^{2+}$  precipitate granules within lipid droplets and (2) the relative cytoplasmic density of lipid in NE cells in the developing midbrain of stages 5–9 chick embryos. Photographic montages of thin, transverse sections through the developing midbrain region were prepared<sup>12</sup>. Measurements of the total areas of the cytoplasm and profiles of lipid droplets in each region (floor, lower walls, and midlateral walls) of the forming NT were taken and the relative cytoplasmic density of lipid (total area of lipid droplets/total cytoplasmic area) was calculated for each region. Separate measurements were made on the apical, neck and basal regions of NE cells to reveal intracellular variations in the cytoplasmic density of lipid. In addition,  $\text{Ca}^{2+}$  precipitate granules were counted and the density of granules within lipid droplets was calculated.

### Results and discussion

The ultrastructural preservation of NE cells prepared by the fluoride-antimonate technique<sup>15</sup> was found to be quite good and comparable to those prepared by more



Figures 1–4. Electron micrographs of contrasted (stained with uranyl acetate and lead citrate) transverse sections through NE cells of stages 5–9 chick embryos that were processed for  $\text{Ca}^{2+}$  localization using the fluoride-antimonate technique<sup>15</sup>.  $\text{Ca}^{2+}$  precipitate (arrows) is most prominent in lipid droplets (L) and appears as small, irregularly shaped electron-dense granules. 1) In neural plate cells of a stage 5 chick embryo, nearly all lipid droplets (L) contain some  $\text{Ca}^{2+}$  precipitate (arrows). Lipid droplets in the apex (2) of NE cells at the point of bending of the V-shaped neuroepithelium are smaller and possess  $\text{Ca}^{2+}$  precipitate denser than those in the cell base (3). 4) In NE cells forming the floor of the midbrain region of a stage 8 embryo, lipid droplets in the apical regions are generally smaller and contain denser  $\text{Ca}^{2+}$  precipitate than those seen in earlier developmental stages. Lu, lumen; Y, yolk. (1)  $\times 16,500$ ; (2)  $\times 18,000$ ; (3)  $\times 8,900$ ; (4)  $\times 16,000$ .

Figure 5. Electron micrograph of an uncontrasted, longitudinal section through mouse skeletal muscle that was processed for  $\text{Ca}^{2+}$  localization using the fluoride-antimonate technique<sup>15</sup>.  $\text{Ca}^{2+}$  precipitate (arrows) is localized almost exclusively within the sarcoplasmic reticulum. M, mitochondria; Z, Z-line; T, T-tubule.  $\times 27,900$ .

Figure 6. Uncontrasted section through the neck region of chick NE cells after processing for  $\text{Ca}^{2+}$  localization and treatment with EGTA. Very little  $\text{Ca}^{2+}$  precipitate is detectable in these sections. L, lipid droplet; M, mitochondria.  $\times 9,700$ .

Figures 7–9. Electron micrographs of uncontrasted thick (1  $\mu\text{m}$ ) sections through the neck regions of NE cells forming the floor of the midbrain region of a stage 8 chick embryo (7 and 8) and a day 9 mouse embryo (9) after processing for  $\text{Ca}^{2+}$  localization using the fluoride-antimonate technique<sup>15</sup>. 7) Lipid droplets (L), a substantial portion of which are contained within the section, show a rather uniform distribution of  $\text{Ca}^{2+}$  precipitate (arrows). RER, rough endoplasmic reticulum; M, mitochondria.  $\times 22,000$ . 8) Reverse contrast imaging accentuates the electron density of the  $\text{Ca}^{2+}$  precipitate against a background provided by the cytoplasmic ground substance. M, mitochondria.  $\times 22,000$ . 9) Section through the perinuclear region of mouse NE cells. Lipid droplets (L) in mouse cells are, for the most part, similar to those in the chick. One notable difference is that some lipid droplets exhibit a more electron-lucent peripheral layer with an irregular perimeter and abundant  $\text{Ca}^{2+}$  precipitate (arrows). M, mitochondria; Nu, nucleus.  $\times 14,900$ .

conventional fixation protocols. In thin transverse sections through NE cells from all phases of neurulation, the cellular location of  $\text{Ca}^{2+}$  is revealed by the presence of small, irregularly shaped, electron-dense granules ( $\text{Ca}^{2+}$ -specific precipitate). These granules are particularly abundant and distributed throughout lipid droplets (figs 1–4). The presence of  $\text{Ca}^{2+}$  within these precipitates was confirmed by the findings that 1) the same cytochemical reaction yields the expected, well-known, distribution pattern of  $\text{Ca}^{2+}$  in and around the sarcoplasmic reticulum of mouse skeletal muscle (fig. 5) and 2) lipid droplets are nearly devoid of  $\text{Ca}^{2+}$  precipitate in NE cells after a brief exposure to EGTA (fig. 6). Furthermore, the possibility that precipitate granules form nonspecifically in lipid droplets is unlikely since, as described below, consistent, region-specific variations in the density of precipitate were observed. In sections contrasted with uranyl acetate and lead citrate to enhance the visualization of general cytoplasmic ultrastructure (e.g. figs 1–4),  $\text{Ca}^{2+}$  precipitate is often difficult to distinguish from other granular, electron-dense, cytoplasmic components (especially ribosomes). To circumvent this problem, the amount and distribution of cytosolic  $\text{Ca}^{2+}$  precipitate was studied in uncontrasted sections (figs 7–9). Figures 7 and 8 show the distribution of  $\text{Ca}^{2+}$  precipitate in thick (1  $\mu\text{m}$ ), uncontrasted sections taken through chick NE cells and examined with a Zeiss CEM 902 electron microscope. These sections contain a roughly 10-fold greater volume of cytoplasm than the thin sections commonly used for transmission electron microscopy and provide a much more reliable depiction of the distribution of  $\text{Ca}^{2+}$  precipitate within lipid droplets and the surrounding cytosol. These sections show that  $\text{Ca}^{2+}$  precipitate is abundant and rather uniformly distributed within individual lipid droplets, but sparse throughout the cytosol (figs 7–8). In addition, examination of thin, uncontrasted sections through the developing NT of mouse embryos shows that  $\text{Ca}^{2+}$  precipitate has the same distribution as that described for the chick NT (fig. 9). The fact that nonmuscle cells generally have low cytosolic  $\text{Ca}^{2+}$  concentrations in the range of  $10^{-7}$  molar, and a total  $\text{Ca}^{2+}$  concentration in the range of a few millimoles per liter has been well-documented<sup>17</sup>. The sparse cytosolic  $\text{Ca}^{2+}$  precipitate that we observed in NE cells is consistent with these findings. No significant regional variations in the amount of cytosolic  $\text{Ca}^{2+}$  precipitate were detected within NE cells. However, we did observe marked variations in the density of  $\text{Ca}^{2+}$  precipitate contained within lipid droplets of NE cells. In fact, although these lipid droplets are found throughout NE cells, a generalized apico-basal gradient in the density of  $\text{Ca}^{2+}$  precipitate is observed within NE cells in which lipid droplets in the cell apex and neck (e.g. figs 1–2) contain a more dense  $\text{Ca}^{2+}$  precipitate than those situated in the cell base (table; fig. 3).

The present study also shows that lipid droplets containing  $\text{Ca}^{2+}$  precipitate are found in NE cells throughout

#### Density of $\text{Ca}^{2+}$ precipitate within lipid droplets<sup>a</sup>

A) Apical lipid vs basal lipid	
Apex	163 $\pm$ 64 <sup>b</sup>
Base	71 $\pm$ 40
B) Apical lipid: Bending region vs non-bending region	
Bending	181 $\pm$ 58 <sup>b</sup>
Non-bending	135 $\pm$ 64

<sup>a</sup> Density expressed as number of precipitate granules/ $\mu\text{m}^2$ .

<sup>b</sup>  $p < 0.01$  by t-test.

the neuroepithelium at all phases of NT formation. Furthermore, the density of  $\text{Ca}^{2+}$  precipitate within individual lipid droplets depends on the location of the lipid droplet within the cell (i.e. apex, neck or base), the specific position of the NE cell within the neuroepithelium (i.e. floor, lower walls or midlateral walls), and whether or not the neuroepithelium exhibits bending at this particular site. For example, in NE cells of the neural plate, nearly all lipid droplets contain some  $\text{Ca}^{2+}$  precipitate, but there are no apparent region-specific differences in the density of  $\text{Ca}^{2+}$  precipitate within or among NE cells. However, at sites where the neuroepithelium exhibits bending, lipid droplets in the apical ends of NE cells clearly contain a denser  $\text{Ca}^{2+}$  precipitate and more prominent precipitate granules than those located in regions that are not engaged in bending (table; figs 1–2 and 4). The finding of  $\text{Ca}^{2+}$  associated with lipid in NE cells is somewhat surprising, but not unprecedented. There is substantial experimental evidence for lipid- $\text{Ca}^{2+}$  associations in other developing systems such as cartilage, bone and dentin<sup>18–21</sup>, and there are a number of proteins (e.g. calmodulin) that, upon binding  $\text{Ca}^{2+}$ , expose hydrophobic domains that can associate with lipid<sup>22</sup>.

Most cellular  $\text{Ca}^{2+}$  has been found to be bound to or enclosed by membranes. For example, a class of smooth vesicles, referred to as calciosomes, has been described in many types of cells that may function as a rapidly exchanging, membrane-enclosed,  $\text{Ca}^{2+}$  pool<sup>23</sup>. A number of studies on the biochemical aspects of NT closure has implicated the key role played by apical microfilament bundles in generating motive forces for this important developmental event. These microfilaments appear to engage in a contractile activity that results in the slow, progressive, apical constriction of NE cells<sup>24,25</sup>. Although the role of  $\text{Ca}^{2+}$  in the regulation of relatively rapid cellular motile activities is rather well-documented<sup>2–4</sup>, how  $\text{Ca}^{2+}$  might regulate the slow, but progressive, contractile activities of microfilament bundles, such as those in NE cells and in the cleavage furrow of dividing cells, remains to be elucidated. In the case of NE cells, we propose here that lipid droplets may be involved in regulating the contractile activity of apical microfilament bundles by mediating a slow, but continual, release of  $\text{Ca}^{2+}$  into the apical cytosol. Although a specific  $\text{Ca}^{2+}$ -releasing mechanism may exist, it is possible that stored

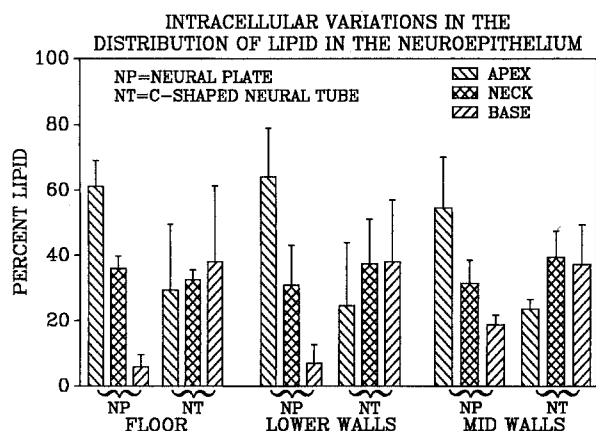


Figure 10. Graph showing the temporal relationship between the cytoplasmic density of lipid in NE cells and local changes in the shape of the neuroepithelium. Morphometric measurements were made on the floor, lower walls and midlateral walls of the neural plate and closed NT. (a) At the neural plate stage, most of the intracellular lipid is concentrated in the apical end of NE cells. By the time the NT has closed, the lipid distribution is more uniform in NE cells.

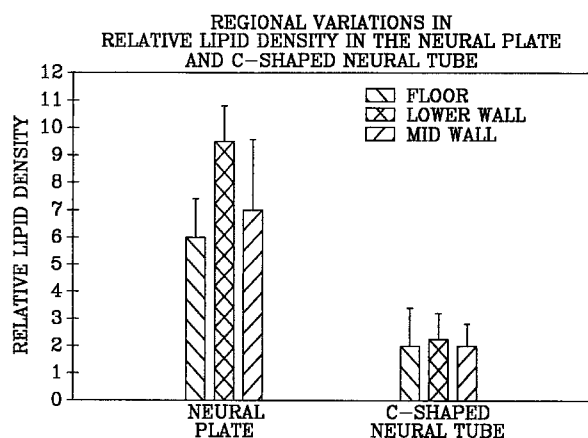


Figure 11. Graph showing the marked reduction in the total amount of lipid in the floor, lower walls and midlateral walls during transformation of the neural plate into a NT.

$\text{Ca}^{2+}$  is gradually liberated from lipid droplets through a rather simple and straightforward mechanism, i.e., utilization of lipid droplets as an energy source<sup>26-28</sup>. Morphometric measurements investigating a possible temporal relationship between the cytoplasmic density of lipid in NE cells and local changes in the overall shape of the neuroepithelium show that NT formation is accompanied by a pronounced change in the relative intracellular distribution of lipid. Results show that, throughout the neural plate, 55–64% of the total intracellular lipid is concentrated within the apical third of NE cells, whereas 31–39% is in the cell neck and 6–19% in the base (fig. 10). A dramatic reduction in the apical lipid and an increase in lipid in the cell base results in a more uniform lipid distribution throughout NE cells of the floor, lower walls and midlateral walls in the C-shaped NT. Despite

this apparent redistribution of intracellular lipid, figure 11 shows that, overall, the total amount of lipid in the floor, lower walls and midlateral walls is sharply reduced during transformation of the neural plate into a C-shaped neuroepithelium. Even though utilization of lipid droplets (and the consequent release of stored  $\text{Ca}^{2+}$ ) may occur throughout NE cells, the loss of  $\text{Ca}^{2+}$  situated in the cell apex would be most likely to have the greatest influence on the contractile activity of apical microfilament bundles, apical constriction of NE cells, and bending of the neuroepithelium. Although our findings raise the possibility that lipid droplets serve as important intracellular  $\text{Ca}^{2+}$  storage sites in NE cells during NT formation, additional work is needed to further clarify the precise role of lipid droplets in  $\text{Ca}^{2+}$  storage and release within the developing neuroepithelium.

- This study was supported by grants from the NIH (NS23200), the BRSG fund of UMDNJ, and the Busch Fund of Rutgers University. Dr Bush was supported by a New Jersey State Postdoctoral Fellowship.
- Hitchcock, S. E., *J. Cell Biol.* 74 (1977) 1.
- Means, A. R., Tash, J. S., and Chafouleas, J. G., *Physiol. Rev.* 62 (1982) 1.
- Campbell, A. K., *Intracellular Calcium: Its Universal Role as a Regulator*. Wiley, New York 1983.
- Carafoli, E., *A. Rev. Biochem.* 56 (1987) 395.
- Ratan, R. R., Maxfield, F. R., and Shelanski, M. L., *J. Cell Biol.* 107 (1988) 993.
- Nagele, R. G., and Lee, H., *J. exp. Zool.* 213 (1980) 391.
- Sadler, T. W., Greenberg, D., Coughlin, P., and Lessard, J. L., *Science* 215 (1982) 172.
- Lee, H., and Nagele, R. G., *J. exp. Zool.* 235 (1985) 205.
- Moran, D., *J. exp. Zool.* 8 (1976) 409.
- Moran, D., and Rice, R. W., *Nature* 261 (1976) 497.
- Nagele, R. G., Bush, K. T., Lynch, F. J., and Lee, H., *Anat. Rec.* 231 (1991) 425.
- O'Shea, K. S., in: *Progress in Anatomy*, pp. 35–60. Ed. R. S. Harrison. Cambridge Univ. Press, New York 1981.
- Smedley, M. J., and Stanisstreet, M., *J. Embryol. exp. Morph.* 89 (1985) 1.
- Poenie, M., and Epel, D., *J. Histochem. Cytochem.* 35 (1987) 939.
- Hamburger, V., and Hamilton, H. L., *J. Morph.* 88 (1951) 49.
- Meldolesi, J., Volpe, P., and Pozzan, T., *Trends Neurosci.* 11 (1988) 449.
- Dirksen, T. R., and Martinetti, G. V., *Tissue Int.* 6 (1970) 1.
- Shapiro, I. M., in: *Biological Mineralization*, pp. 117–138. Ed. I. Zipkin. Wiley, New York 1973.
- Boyan, B. D., Schwartz, Z., Swain, L. D., and Khare, A., *Anat. Rec.* 224 (1989) 211.
- Eanes, E. D., *Anat. Rec.* 224 (1989) 20.
- Klee, C. B., *Biochemistry* 16 (1977) 1017.
- Volpe, P., Krause, K. H., Hashimoto, S., Zorzato, F., Pozzan, T., Meldolesi, J., and Lew, D. P., *Proc. natl Acad. Sci. USA* 85 (1988) 1091.
- Nagele, R. G., Bush, K. T., Kosciuk, M. C., Hunter, E. T., Steinberg, A. B., and Lee, H., *Dev. Brain Res.* 50 (1989) 101.
- Bush, K. T., Lynch, F. J., DeNittis, A. S., Steinberg, A. B., Lee, H., and Nagele, R. G., *Anat. Embryol.* 181 (1990) 49.
- Karfunkel, P., *Int. Rev. Cytol.* 38 (1974) 245.
- Paz, P., Zapata, A., Fernandez, J. G., Chamorro, C., and Villar, J. M., *Acta anat.* 124 (1985) 227.
- Fernandez, J. G., Chamorro, C. A., De Paz, P., and Villar, J. M., *J. exp. Zool.* 245 (1988) 17.